Journal of Rainwater Catchment Systems Vol.14/No.1/pp.17-24

Journal of Rainwater Catchment Systems

# Numerical Modeling of Seawater Intrusion Management Measures

Mary Makokha [1], Akira Kobayashi [2] and Shigeyasu Aoyama [3]

**Abstract:** Overexploitation of coastal aquifers has become a common issue with many coastal regions experiencing extensive seawater intrusion, resulting in severe deterioration of groundwater quality. When analyzing the freshwater quality extracted from the pumping wells in coastal aquifers, the movement of very low concentrations of the solute is critical in analyzing the level of contamination in pumping wells. This research analyzes the effectiveness of four seawater control measures using a hypothetical steady-state salt distribution model in a representative cross-section perpendicular to the coastline using a two-dimensional density-dependent solute transport model through homogeneous media. It is established that the shallow pumping wells are more preferable than the deep pumping wells as they have relatively lower concentration value in the pumping well. Low permeable aquifers give high concentration values in the pumping well and the extent of seawater intrusion is large than the high permeable ones. The level of contamination in the pumping well is proportional to the extent of seawater intrusion wedge. Pumping wells located further away from the seashore are not affected by the presence of the seawater intrusion wedge; however, this may not be an effective method of controlling seawater intrusion. Deep recharge wells closer to the pumping well seem to be the most effective method of controlling the extent of seawater intrusion and the concentration value in the pumping well. Deep seawater pumping wells located relatively away from the pumping well could be used to control seawater intrusion if proper disposal methods for the extracted saltwater are implemented. Low permeable barrier walls located closer to the pumping well could be used, although the initial cost of construction may be high.

***Keywords:*** *Seawater intrusion; Concentration; Pumping wells; Numerical modeling; Control measure*

## 1 Introduction

In many coastal aquifers, intrusion of seawater has become one of the constraints affecting groundwater management. The coastal areas of the world are characterized by high populations, with about 70% of the world's population living within 60 km of the shoreline and eight of the 10 largest cities in the world are located along the coastline (Oude Essink, 2001). Overexploitation of these coastal aquifers has become a common issue with many coastal regions experiencing extensive seawater intrusion, resulting in severe deterioration of ground freshwater quality. As seawater intrusion progresses, existing pumping wells, especially close to the coast, become saline due to upconing and they are abandoned. Management of these coastal aquifers in such situations is a delicate task and requires special attention to minimize the movement of the seawater wedge into aquifers and up-coning of seawater near pumping stations (Reilly and Goodman, 1987 and Bower et *al.*, 1999). The rate of abstraction in pumping wells along the coastal areas should not exceed the permissive sustainable yield. Prevention of salinisation becomes critical and detailed characterization of coastal aquifers is quite essential for prevention and remediation to protect coastal aquifers from seawater intrusion.

The extent of intrusion depends on a number of factors such as aquifer geometry and properties, abstraction rates, depth, recharge rate and distance of pumping wells from the coastline (Ghassemi *et al.*, 1993). Complex models are required to quantify these factors, so that proper control measures are undertaken to control seawater intrusion. Numerical modeling is a powerful tool for the parameterization and validation of comprehensive coastal aquifer management (Van Dam, 1993; Oude Essink, 1996). This research analyzes the effectiveness of different seawater control measures using a hypothetical steady-state salt distribution model in a representative cross-section perpendicular to the coastline using a two-dimensional density-dependent solute transport model through homogeneous media. The aquifer is assumed to consist of a single homogeneous porous medium with the impervious bottom being horizontal.

When analyzing the freshwater quality extracted from the pumping wells affected by seawater intrusion, the movement of very low concentrations of the solute is critical with respect to water supply in pumping wells. The normalized concentration is important in defining the level of contamination in pumping wells.

The seawater intrusion control methods analyzed include the location of pumping wells (*PW*), the use of Recharge wells (*RW*), Seawater pumping wells (*SWPW*), and barrier system. Previous research done by Van Dam (1993), revealed that these methods could be used to control seawater intrusion in coastal areas. The technical and environmental limits posed by the probable control measures in an aquifer system are also discussed. This was quite essential in proposing the ultimate location of the pumping wells in terms of the technical and environmental aspects within the prevailing physical constraints.

[1]Ph.D. Student, Graduate School of Agriculture, Kyoto University, Kitashirakawa-Oiwake-cho, Sakyo-ku, Kyoto 606-8502, Japan, (Corresponding Author) E-mail; makokha@yahoo.com

[2] Associate Professor, Graduate School of Agriculture, Kyoto University, Kitashirakawa-Oiwake-cho, Sakyo-ku, Kyoto 606-8502, Japan

[3]Professor, Environmental Science Division, Ishikawa Prefectural University, Nonoichi-cho, Ishikawa 921-8836, Japan

## 2 Numerical Modeling

### 2. 1 Numerical Theory

The governing equations used in the analysis were given by:

$$S_s \frac{\partial H_f}{\partial t} = \frac{\partial}{\partial x_i}\left\{ \frac{K_{ij}}{1+\beta_\mu \overline{C}} \left( \frac{\partial H_f}{\partial x_j} + \frac{\rho_f}{\rho} \varepsilon_c \overline{C} \delta_{j2} \right) \right\} \quad (1)$$

$$R_d n \frac{\partial \overline{C}}{\partial t} = \frac{\partial}{\partial x_i}\left\{ D_{ij} \frac{\partial \overline{C}}{\partial x_j} - V_i \overline{C} \right\} \quad (2)$$

where $H_f$ is the total head of freshwater, $S_s$ is the specific storage, $K_{ij}$ is the hydraulic conductivity tensor of freshwater, $\varepsilon_c$ is the dimensionless density reference ratio defined as; $\varepsilon_c = \rho_{max}/\rho_f - 1$, in which $\rho_f$ is the freshwater density, $\overline{C}$ is the normalized concentration defined as $\overline{C} = C/C_{max}$ ,where $C_{max}$ is concentration corresponding to the maximum fluid density $\rho_{max}$ , $C$ is the concentration, $\delta_{ij}$ is the Kronecker's delta, $t$ is time, $R_d$ is the retardation factor, $V_i$ is Darcy's velocity vector, $x_i$ is the location vector, $t$ is the time and $D_{ij}$ is the dispersion coefficient tensor defined as;

$$D_{ij} = \begin{cases} a_T |V| + (a_L - a_T) V_i^2 / |V| & if\ i = j \\ (a_L - a_T) V_i V_j / |V| & if\ i \neq j \end{cases} \quad (3)$$

where $a_L$ is the longitudinal dispersivity and $a_T$ is the transversal one. In (1), $i = j = 2$, is vertical.

In addition $\beta_\mu$ is defined as;

$$\beta_\mu = \frac{1}{\mu_f} \frac{\partial \mu}{\partial \overline{C}} \quad (4)$$

in which $\mu_f$ is the viscosity of freshwater, $\mu$ is the dynamic viscosity of the fluid and $\beta_\mu$ is the ratio of change in viscosity with reference to concentration. For (1) and (2), the summation convention is applied for the direction, $i$ and $j$. (1) is the continuity equation of groundwater and (2) is the solute mass balance equation. (1) was derived from assuming two driving forces of the piezometric head gradient and the buoyancy force directed vertically upward. The normalized concentration of the second term on the right hand side is treated as an unknown variable, while the one in the viscosity term related to the hydraulic conductivity tensor is treated as a known value using the one at the previous iteration step. In (2), the Darcy's velocity, $V_i$ is also treated as a known value by using the one at the previous iteration step. Therefore (1) has two unknown variables; $H_f$ and $\overline{C}$ and (2) has one unknown variable $\overline{C}$ . Therefore two unknown variables are solved from the simultaneous equations. Considering the change in viscosity and velocity, the iteration calculation is carried out. The governing equations are solved using the finite element method, in which the ordinary shape function is used. The special treatment for stability in the case of the large advection is not considered, since the velocity analyzed in this study is not expected to be so high. Actually there are no oscillations in the results. Since the total head of the freshwater $H_f$ is an unknown variable, the boundary condition at the downstream side, which is the total head of saltwater $H_s$ is fixed and has to be modified using the following equation;

$$H_f = z + (1 + \varepsilon_c)(H_s - z) \quad (5)$$

After solving the equation at steady state conditions, the concentration in the pumping well is also examined at steady state conditions.

### 2.2 Model Description

The two dimensional cross-section for the coastal aquifer system has a flow domain of A-B-C-D-E as shown in Figure 1. The model dimensions are; width of 60m and height of 30m.

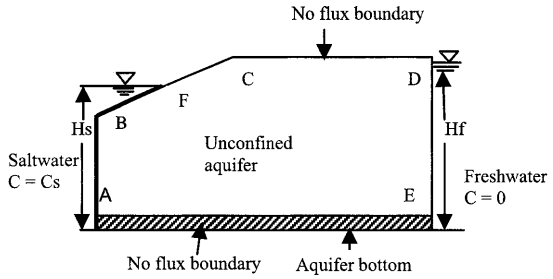


Figure 1: Crossection through unconfined aquifer

Along the no flux boundaries; CD and AE, the total flux perpendicular to the boundary is zero. Along the slope BC, the concentration $\overline{C}$ is constant and constant total head $H_s$ is set up to the node of which the elevation coincided with the salt water level as indicated by the thick line BF on the slope in Figure 1. Zero flux condition is applied on the nodes over the saltwater level as shown by the thin line on the slope FC. Along the boundary AB and DE, constant head and concentration were applied. In Figure 1, the sea shore is defined as position F.

The finite representation of the system comprised of 1781 nodes and 1700 elements. The general flow and transport parameters for all cases were as in Table 1. Since the parameter $\beta_\mu$ has not been studied well, the value was tentatively set as shown in Table 1. The values are assumed hypothetically and the parametric study about hydraulic conductivity is carried out. In this study, the hydraulic conductivity is assumed to be isotropic, while the diffusivity is considered to be anisotropic. Since the simulation is carried out at steady state conditions, the specific storage and the retardation factor are not necessary for the simulation.

Table 1: Flow and transport parameters for numerical model

| Parameters | Values and Units |
|---|---|
| Pumping rate of pumping well ($q_p$) | $5 \times 10^{-3}$ ms$^{-1}$ |
| Porosity ($n$) | 0.33 |
| Freshwater concentration | 0 % |
| Seawater concentration | 3 % |
| Modified coefficient of viscosity( $\beta_{\mu}$ ) | 0.01 |
| Density reference ratio ( $\varepsilon_c$ ) | 0.03 |
| Longitudinal diffusivity ( $\alpha_L$ ) | $2 \times 10^{-2}$ m |
| Transverse diffusivity ( $\alpha_T$ ) | $2 \times 10^{-3}$ m |

### 2.3 Description of the seawater control measures

Four seawater control measures were analyzed namely; the location of pumping wells (*PW*) from the sea shore, the use of recharge wells (*RW*), seawater pumping wells (*SWPW*) and the barrier system. The normalized concentration $\overline{C}$ , in the pumping wells was calculated considering all the methods. The pumping wells used were located at a depth of 10 m, 16 m, and 26 m. They were at a horizontal distance of 6m from the sea shore. The pumping rate was described at the node corresponding to the depth of *PW*.

Table 2 shows the specific parameters used to model the four control measures. In the first method the *PW* were located at a varying horizontal distance from the sea shore. The discharge index ($Q$) was calculated and it was defined by; $Q = KiLd/q_p$ where $K$ is the hydraulic conductivity assumed to be isotropic, $i$ is the average hydraulic gradient of the region calculated from the boundary conditions and was a constant of about 0.02, $L$ is the horizontal distance of the pumping well from the sea shore, $d$ is the depth of the pumping well and $q_p$ is the pumping rate. If the $Q$ value is small, the pumping well suffers greatly from the effect of seawater intrusion. This index is only applied in the examination of location of pumping well.

Recharge wells (*RW*) are used to inject freshwater into an aquifer for primary purposes of controlling seawater intrusion to protect coastal aquifers from contamination. They are located in the upstream of the pumping well. A constant total head equal to the ground level was fixed for all the nodes in the recharge well. Total recharge flux of the recharge well was then calculated. Seawater pumping wells (*SWPW*) are used to extract saltwater along the coast in order to reduce the length of seawater intrusion and prevent coastal aquifers from contamination. They are located downstream of the pumping well in the sea. The seawater barrier walls are used to protect the pumping wells from contamination. The effect of varying the permeability of the barrier and length were analyzed. For all the control measures, $K$ is applied to $K_{xx}$ and $K_{zz}$ direction, $K_{xz}$ is set at zero.

Table 2: Parameters for four control measures

| Method | Parameters |
|---|---|
| *a*)Location of *PW* | |
| Depth of *PW* | 10, 16, 26 m |
| Horizontal distance of *PW* from sea shore | 4, 6, 8, 10, 12, 28 m |
| Hydraulic conductivity ($K$) | $2.4\times10^{-3}$, $4.7\times10^{-3}$, $7.1\times10^{-3}$ ms$^{-1}$ |
| Pumping rate ($q_p$) | $5.0\times10^{-5}$ m$^3$s$^{-1}$ |
| *b*) Recharge wells (*RW*) | |
| Depth of *RW* | 4, 10, 13, 26 m |
| Horizontal distance of *RW* from *PW* | 4, 12 m |
| Hydraulic conductivity ($K$) | $4.7\times10^{-3}$ ms$^{-1}$ |
| *c*) *SWPW* | |
| Depth of *SWPW* | 4, 10, 13, 26 m |
| Distance of *SWPW* from *PW* | 2, 5, 8 m |
| Hydraulic conductivity ($K$) | $4.7\times10^{-3}$ ms$^{-1}$ |
| Pumping rate ($q_p$) | $2.0\times10^{-3}$, $2.5\times10^{-3}$ m$^3$s$^{-1}$ |
| *d*) Barrier System | |
| Length of barriers | 15, 20 m |
| Distance of barrier from *PW* | 2 , 4 m |
| Hydraulic conductivity of barrier | $4\times10^{-4}$, $4\times10^{-8}$ ms$^{-1}$ |

## 3 Results and analysis

### 3.1 Location of pumping wells and pumping rate

Table 3 shows the results obtained for varying the horizontal distance of the pumping wells from the sea shore for the case of $K = 4.7\times10^{-3}$ ms$^{-1}$.

Table 3: Discharge Index ($Q$) and normalized concentration ($\overline{C}$) values for $K$ =4.72 $\times10^{-3}$ ms$^{-1}$

| Horizontal distance of *PW* from shore (m) | Depth (m) | $Q$ | $\overline{C}$ |
|---|---|---|---|
| 4 | 10 | 3.68 | 0.23 |
| | 16 | 2.58 | 0.29 |
| | 26 | 0.73 | 0.37 |
| 6 | 10 | 4.51 | 0.20 |
| | 16 | 3.16 | 0.25 |
| | 26 | 0.90 | 0.31 |
| 8 | 10 | 5.33 | 0.16 |
| | 16 | 3.73 | 0.21 |
| | 26 | 1.06 | 0.27 |
| 10 | 10 | 6.56 | 0.11 |
| | 16 | 4.59 | 0.17 |
| | 26 | 1.31 | 0.21 |
| 12 | 10 | 6.97 | 0.15 |
| | 16 | 4.88 | 0.16 |
| | 26 | 1.39 | 0.19 |
| 28 | 10 | 11.49 | 0.00 |
| | 16 | 8.04 | 0.00 |
| | 26 | 2.29 | 0.00 |

It was observed that the discharge index varied inversely with the concentration; that is, the concentration increased with depth of the *PW*. Shallow *PW* of 10 m depth had less $\overline{C}$ value than deep *PW* of 26 m.

Figure 2 shows the relationship between discharge index and the $\overline{C}$ value in *PW* located at different horizontal positions. The $\overline{C}$ value seemed to decrease as the horizontal distance from the shore increased from 4 m to 12m. This could also be seen from Figure 2 as the gradient of the $\overline{C}$ was steep for *PW* near the sea shore at 4 m and it reduced gradually for *PW* that were 12 m away from the sea shore.

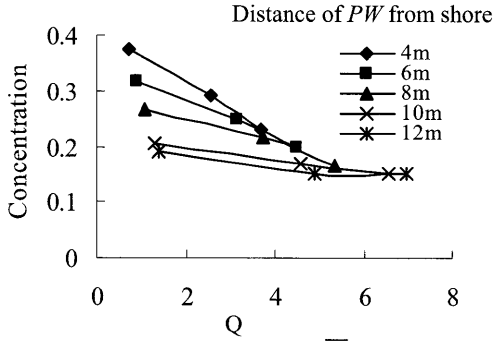


Figure 2: Normalized concentration ($\overline{C}$) and discharge index (Q) in the *PW* at 10 m depth

The wells located 28 m away from the sea shore were not affected by the seawater intrusion as they had $\overline{C}$ values equals to zero.

Varying the hydraulic conductivity also had an effect on the $\overline{C}$ value in the pumping wells. Table 4 shows the discharge index and the $\overline{C}$ values at varying hydraulic conductivity. High $\overline{C}$ values were observed in the case of $K = 2.4\times10^{-3}$ ms$^{-1}$, compared to the case of hydraulic conductivity was $K = 7.1\times10^{-3}$ ms$^{-1}$. The seawater intrusion was relatively less in the case of $K = 7.1\times10^{-3}$ ms$^{-1}$ Compared to the case of $K = 2.4\times10^{-3}$ ms$^{-1}$. Large intrusion meant high $\overline{C}$ values in the *PW*. Therefore the hydraulic conductivity and the horizontal distance of *PW* from the sea shore affect the $\overline{C}$ value in *PW*.

Table 4: Discharge Index ($Q$) and ($\overline{C}$) values for varying hydraulic conductivity ($K$)

| $K$ (ms$^{-1}$) | | $2.4\times10^{-3}$ | | $7.1\times10^{-3}$ | |
|---|---|---|---|---|---|
| Distance of *PW* from shore (m) | Depth (m) | $Q$ | $\overline{C}$ | Q | $\overline{C}$ |
| 4 | 10 | 1.85 | 0.32 | 5.53 | 0.15 |
| | 16 | 1.29 | 0.40 | 3.87 | 0.23 |
| | 26 | 0.37 | 0.45 | 1.10 | 0.32 |
| 6 | 10 | 2.25 | 0.29 | 6.77 | 0.14 |
| | 16 | 1.57 | 0.35 | 4.73 | 0.18 |
| | 26 | 0.45 | 0.40 | 1.35 | 0.26 |
| 8 | 10 | 2.66 | 0.26 | 8.00 | 0.11 |
| | 16 | 1.86 | 0.31 | 5.59 | 0.07 |
| | 26 | 0.53 | 0.35 | 1.59 | 0.21 |
| 10 | 10 | 3.28 | 0.23 | 9.85 | 0.01 |
| | 16 | 2.29 | 0.26 | 6.89 | 0.02 |
| | 26 | 0.65 | 0.29 | 1.96 | 0.06 |
| 12 | 10 | 3.48 | 0.22 | 10.47 | 0.01 |
| | 16 | 2.44 | 0.24 | 2.44 | 0.01 |
| | 26 | 0.69 | 0.27 | 0.69 | 0.02 |
| 28 | 10 | 5.74 | 0.06 | 17.22 | 0.00 |
| | 16 | 4.01 | 0.10 | 12.05 | 0.00 |
| | 26 | 1.14 | 0.11 | 3.44 | 0.00 |

Figure 3 shows the relationship of $\overline{C}$ and $Q$ in relation to the varying $K$ for the *PW* located at 10 m depth. High $Q$ values were observed in the case of high $K$ values. From the $Q$ value the contamination in the pumping well could be inferred; High Q value meant low $\overline{C}$ value in *PW*. Therefore shallow *PW* located at 10 m depth and at a horizontal distance of 28 m were most effective in reducing the $\overline{C}$ value in the *PW*.

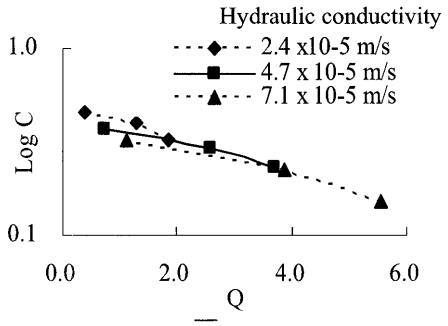


Figure 3: Relationship of $\overline{C}$ value and $Q$ in *PW* at 10 m with varying hydraulic conductivity ($K$)

### 3.2 Recharge wells (*RW*)

For all the cases, to examine the effect of *RW*, the *PW* existed at the distance of 6 m from the seashore.

Table 5 shows the results for varying the horizontal distance and depth of *RW* for the *PW*. The results reveal that as the depth of the *RW* is increased the $\overline{C}$ value of water in *PW* reduced, that is, they are inversely proportional. Figure 4 shows the relationship between the $\overline{C}$ value in the *PW* of 16 m depth, and the depth and the horizontal distance of the *RW*. The same tendency was observed in the different depth of the *PW*. Deep *RW* significantly reduced the $\overline{C}$ value in the *PW*. When the *RW* was located 26 m deep, the value of $\overline{C}$ in *PW* was zero. The $\overline{C}$ values were relatively higher when the *RW* was 4 m deep (Table 5). *RW* located 4 m away from the *PW* seemed to effectively reduce the $\overline{C}$ value in *PW* than the *RW* located 12 m away.

Figure 5 shows the relationship between the depth and the total recharge flux ($q$) of the *RW* in the case of *PW* at 16 m depth. The same tendency between the depth and $q$ in the *RW* was observed for the different depth of the *PW*. The total $q$ increased as the depth of the *RW* increased; they are directly proportional. The total recharge flux reduced as the *RW* were located from 4 m to 12 m from the *PW*. This implies that a lot of recharge flux is required for *RW* located 4 m away from the *PW* than the *RW* located 12 m away to maintain the groundwater total head. The $q$ value was inversely proportional to the $\overline{C}$ value in the *PW*; that is, high $q$ values implied low $\overline{C}$ values in the *PW*.

Figure 6 shows the $\overline{C}$ distribution for *RW* at varying depth. The extent of the seawater intrusion wedge was significantly reduced when the *RW* was located 26 m deep than when it was at 4 m depth. The depth of the *RW* is inversely proportional to the extent of intrusion wedge. Therefore the deep *RW* that is closer to the *PW* seems to be the most effective method in reducing the extent of the seawater intrusion wedge and the $\overline{C}$ value in the *PW*.

Table 5: Effects of horizontal distance and depth of *RW* on the $\overline{C}$ value in the *PW*

| Distance of *RW* from *PW* | | 4 m | | 12 m | |
|---|---|---|---|---|---|
| Depth of *PW* (m) | Depth of *RW* (m) | $\overline{C}$ | $q$ | $\overline{C}$ | $q$ |
| 10 | 26 | 0.000 | 0.010 | 0.000 | 0.007 |
| | 13 | 0.002 | 0.008 | 0.005 | 0.005 |
| | 10 | 0.005 | 0.007 | 0.006 | 0.003 |
| | 4 | 0.011 | 0.005 | 0.025 | 0.003 |
| 16 | 26 | 0.000 | 0.010 | 0.007 | 0.007 |
| | 13 | 0.008 | 0.008 | 0.024 | 0.005 |
| | 10 | 0.010 | 0.007 | 0.047 | 0.003 |
| | 4 | 0.098 | 0.005 | 0.168 | 0.003 |
| 26 | 26 | 0.001 | 0.010 | 0.086 | 0.007 |
| | 13 | 0.060 | 0.007 | 0.383 | 0.005 |
| | 10 | 0.171 | 0.006 | 0.458 | 0.003 |
| | 4 | 0.219 | 0.004 | 0.897 | 0.003 |

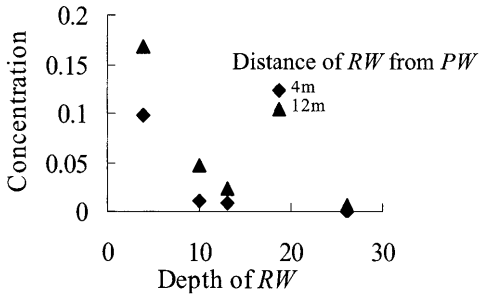


Figure 4: Relationship between $\overline{C}$ value in the *PW* at 16m depth and the horizontal distance and depth of *RW*

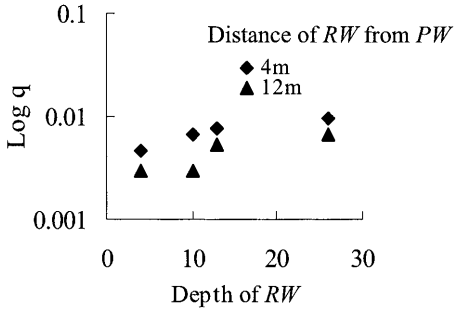


Figure 5: Relationship between $q$ and depth of *RW* in the *PW* at 16m depth

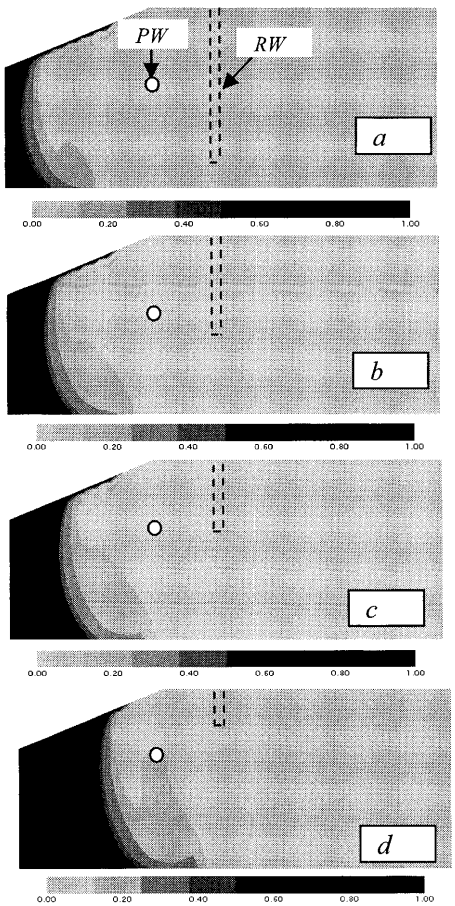


Figure 6: Effect of varying depth of *RW* on the extent of seawater intrusion; *a* is *RW* at 26 m depth; *b* is *RW* at 13 m depth; *c* is *RW* at 10 m depth; *d* is *RW* at 3 m depth located at horizontal distance of 4 m away from 10 m depth *PW*

### 3.3 Sea water pumping wells (*SWPW*)

To examine the effect of the *SWPW*, the *PW* was located at a horizontal distance of 6 m from the seashore.

Table 6 shows the results obtained for varying the horizontal distance, depth, and the pumping rate of *SWPW* on the value of $\overline{C}$ in the *PW*.

It was generally observed that the shallow *PW* had relatively lower $\overline{C}$ values than the deep *PW*. The position of the *SWPW* also affected significantly the value of $\overline{C}$ in the *PW*. For instance, considering the *PW* located at a depth of 10 m, the *SWPW* placed at 26 m depth seemed to effectively reduce the value of $\overline{C}$ in the *PW*. The general trend was that, as the depth of the *SWPW* increased the value of $\overline{C}$ in the *PW* significantly reduced. The $\overline{C}$ value in the *PW* is inversely proportional to the depth of the *SWPW*.

The horizontal distance of the *SWPW* also had an effect on the extent of seawater intrusion and the value of $\overline{C}$ in the *PW*. Figure 7 shows the $\overline{C}$ distribution to indicate the effect of varying the horizontal distance of the *SWPW* from the *PW* on the extent of seawater intrusion. It is observed from Figure 7 and Table 6 that, the *SWPW* located 8 m away reduced significantly the extent of seawater intrusion wedge and the $\overline{C}$ value in the *PW*, than the well at a horizontal distance of 2 m. The extent of seawater intrusion influences the $\overline{C}$ value in the *PW*.

As the horizontal distance of the *SWPW* from the *PW* increased, the $\overline{C}$ value in the *PW*, and the extent of seawater intrusion wedge also reduced. Therefore deep *SWPW* that is located relatively away from the *PW*, is effective in reducing the extent of seawater intrusion wedge and the $\overline{C}$ value in the *PW*.

Lowering the pumping rate by 20 % did not induce the clear increase of the $\overline{C}$ value in the *PW*. This implies that small changes in the pumping rate in the *SWPW*, does not affect the measure of the $\overline{C}$ value in *PW* (Table 6).

Table 6: Effect of depth variation, horizontal distance, and pumping rate of *SWPW* on the $\overline{C}$ value in the *PW*

| *SWPW pumping rate (m3s-1)* | | 2.5 × 10-3 | | | 2 × 10-3 |
|---|---|---|---|---|---|
| Horizontal distance of *SWPW* from *PW* | | 2m | 5m | 8m | 2m |
| Depth of *PW* (m) | Depth of *SWPW* (m) | $\overline{C}$ | $\overline{C}$ | $\overline{C}$ | $\overline{C}$ |
| 10 | 26 | 0.140 | 0.139 | 0.135 | 0.166 |
| | 13 | 0.160 | 0.143 | 0.138 | 0.181 |
| | 10 | 0.229 | 0.211 | 0.198 | 0.240 |
| | 4 | 0.336 | 0.286 | 0.203 | 0.368 |
| 16 | 26 | 0.198 | 0.178 | 0.162 | 0.203 |
| | 13 | 0.361 | 0.232 | 0.200 | 0.373 |
| | 10 | 0.389 | 0.312 | 0.243 | 0.398 |
| | 4 | 0.370 | 0.348 | 0.292 | 0.422 |
| 26 | 26 | 0.170 | 0.148 | 0.165 | 0.197 |
| | 13 | 0.489 | 0.434 | 0.359 | 0.496 |
| | 10 | 0.494 | 0.445 | 0.383 | 0.502 |
| | 4 | 0.500 | 0.416 | 0.385 | 0.525 |

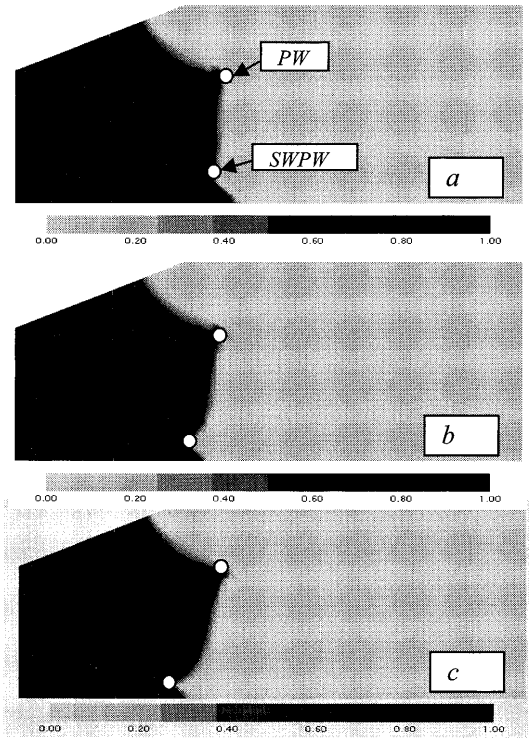


Figure 7: Effect of varying the horizontal distance of the *SWPW* at 26 m depth on the extent of seawater intrusion; *a* is 2 m from *PW*; *b* is 5 m from *PW*; *c* is 8 m from *PW*

### 3.4 Barrier system

To examine the effect of the barrier system, the *PW* was located at a horizontal distance of 6 m from the seashore.

Table 7 shows the results for varying the permeability of the barrier wall on the $\overline{C}$ value in the *PW*. The observed general trend was that, as the depth of the *PW* increased the $\overline{C}$ value also increased; the deep *PW* was more contaminated than shallow *PW*.

Figure 8 shows the $\overline{C}$ distribution indicating the effect of varying the permeability of the barrier on the extent of seawater intrusion wedge for the case of the *PW* located at 10 m depth. The actual length of the barrier was considered to be half of the total length of barrier shown in Table 7. The upper half had the permeability corresponding to that of the porous media. It was observed that when the permeability of the barrier was low the saltwater intrusion wedge went around the barrier. The low permeable barrier reduced the $\overline{C}$ value in the *PW* by almost 42 %; that is, as the permeability of the barrier became low, the $\overline{C}$ value in the *PW* also significantly became low. However the effect of lowering the permeability of the barrier is not proportional to reducing the salinity in the *PW*.

Doubling the horizontal distance of location of the barrier from the *PW* did not seem to change so much the $\overline{C}$ value in the *PW*. The $\overline{C}$ value for the barrier at 4 m increased within the range of 2- 15 % (Table 7). Therefore building barriers further away from the *PW* may not be quite necessary.

Increasing the length of the barrier of $K$= 4.72×10$^{-4}$ ms$^{-1}$ by 33 %, did not also affect so much the $\overline{C}$ value in the *PW*. In the case of $K$=4.72×10$^{-8}$ ms$^{-1}$, the $\overline{C}$ value in the *PW* at 16 m depth, reduced by 6 % and in the *PW* at 26 m depth, the $\overline{C}$ value was reduced by 7 % (Table 7). Therefore when considering using the barrier system as seawater control measure, the permeability of the barrier system seems to have an effect on the reduction of salinity of the *PW*. However the length and location of the barrier may not be quite negligible especially when using a low permeable barrier.

Table 7: Effects of varying the horizontal distance, permeability, and the length of barrier on the $\overline{C}$ the value in the *PW*

| Permeability of barrier (ms$^{-1}$) | $K$=4.72×10$^{-4}$ | | | |
|---|---|---|---|---|
| Length of barrier (m) | 15 | | 20 | |
| Horizontal distance of barrier from *PW* (m) | 2 | 4 | 2 | 4 |
| Depth of *PW* (m) | $\overline{C}$ | $\overline{C}$ | $\overline{C}$ | $\overline{C}$ |
| 10 | 0.178 | 0.180 | 0.169 | 0.169 |
| 16 | 0.235 | 0.240 | 0.223 | 0.221 |
| 26 | 0.305 | 0.308 | 0.303 | 0.295 |
| Permeability of barrier (ms$^{-1}$) | $K$=4.72×10$^{-8}$ | | | |
| Length of barrier (m) | 15 | | 20 | |
| Horizontal distance of barrier from *PW* (m) | 2 | 4 | 2 | 4 |
| Depth of *PW* (m) | $\overline{C}$ | $\overline{C}$ | $\overline{C}$ | $\overline{C}$ |
| 10 | 0.103 | 0.119 | 0.101 | 0.126 |
| 16 | 0.180 | 0.193 | 0.110 | 0.143 |
| 26 | 0.239 | 0.261 | 0.224 | 0.248 |

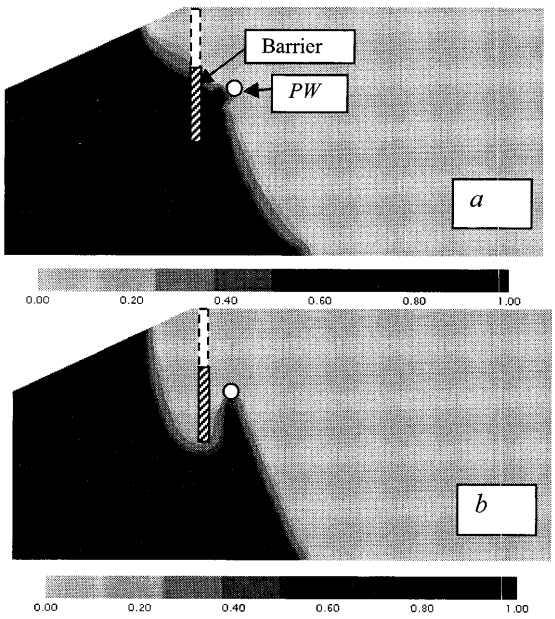


Figure 8: Effect of varying the permeability on the extent of seawater intrusion for the 15 m length barrier, at a horizontal distance of 2 m from the *PW* located 10 m deep; *a* is $K$=4.72 ×10$^{-4}$, *b* is $K$=4.72 × 10$^{-8}$ ms$^{-1}$

## 4 Technical, and environmental aspects of the reviewed control measures

From the foregoing discussion, it is obvious from all the four control measures reviewed that shallow *PW* are more preferable than the deep *PW* as the $\overline{C}$ value is relatively less in the shallow *PW* than the deep *PW*. In addition, the extent of the seawater intrusion wedge affects the $\overline{C}$ value in the *PW*. As the seawater intrusion wedge increases, the $\overline{C}$ value in the *PW* also increases; they are directly proportional. Therefore reducing the extent of the seawater intrusion wedge is primary in reducing the $\overline{C}$ value in the *PW*.

Figure 9 shows the $\overline{C}$ values for the most effective option of each of the four reviewed methods in comparison to the $\overline{C}$ values of the *PW* at a horizontal distance of 6 m from the seashore, before the application of the control measures. Figure 10 shows the extent of the seawater intrusion wedge. Figure 10*a* is the seawater intrusion wedge for the 10 m deep *PW* without the control measures. Figure 10*b* is the one for the *PW* located 28 m away from the seashore. It is observed that, the *PW* which is located further away at 28 m from the seashore is not affected by the seawater intrusion wedge and the $\overline{C}$ value in the *PW* is zero.

The deep *RW* located 4m away from *PW* and 26 m deep significantly reduced the $\overline{C}$ value in the PW to zero (Figure 9). The extent of seawater intrusion was also significantly reduced (Figure 6*a*). However the deep *RW* requires large recharge flux. The large amounts of artificial recharge could be expensive and it may be difficult to maintain the water head required for the *RW*, therefore raising environmental and economic issues. Therefore, when selecting the location of *RW*, it should be deep and close to the *PW*.

The *SWPW* located 8 m away from the *PW* and at a depth of 26 m was effective in reducing the $\overline{C}$ value in the *PW* (Figure 9) and the extent of the intrusion wedge (Figure 7*c*).

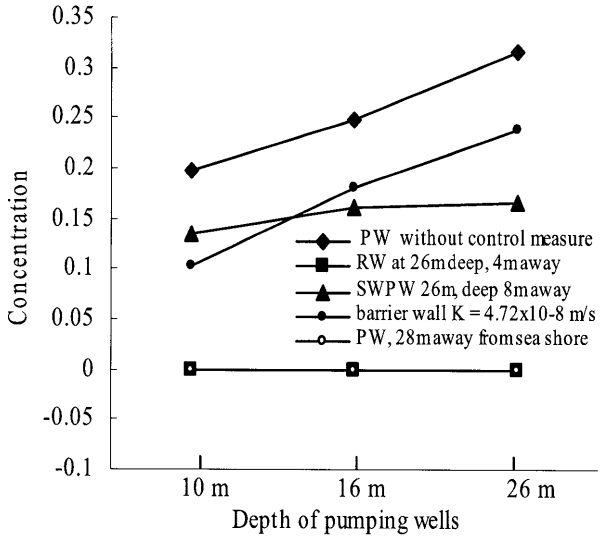


Figure 9: The $\overline{C}$ values of the *PW* for the most effective option of each reviewed method

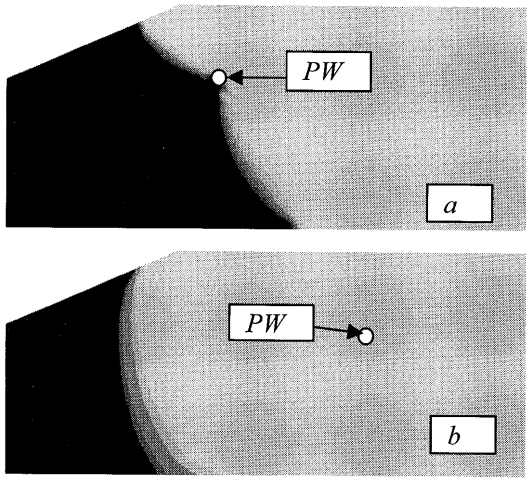


Figure 10: Seawater intrusion wedge; *a* is the *PW*, 10 m deep without the control measures; *b* is locating *PW*, 28 m from sea shore

However the general limitation of this method could be the disposal of the extracted saltwater from the *SWPW* (Todd, 1974). Therefore this method may not be economically and environmentally feasible.

The seawater barrier wall with low permeability ($K$=4.72 $\times$ $10^{-8}$ $ms^{-1}$) and located 2m away from *PW* relatively reduced the $\overline{C}$ value in the *PW* (Figure 9). However since the difference of permeability, location and length of barrier have little effect on the reduction of salinity in the *PW*, an economical barrier should be selected.

## 5 Conclusions

- It is clear from all the four reviewed methods that the shallow *PW* are more preferable than the deep *PW* as the $\overline{C}$ value in the shallow wells is lower.
- The extent of seawater intrusion is proportional to the $\overline{C}$ value in the *PW;* therefore controlling seawater intrusion is very critical in controlling contamination in pumping wells.
- The permeability of an aquifer affects the extent of seawater intrusion and therefore, contamination. Low permeable aquifers have high $\overline{C}$ values and the extent of seawater intrusion is large, than the high permeable aquifers.
- *PW* located further away from the sea shore are not affected by the presence of the seawater intrusion wedge.
- Deep *RW* located closer to the *PW* are the most effective, in reducing the $\overline{C}$ value and the extent of seawater intrusion. However they require large volumes of water to maintain the total head. Therefore it may be expensive to maintain them.
- Deep *SWPW* located relatively away from the *PW* could be used to control seawater intrusion if proper disposal methods for the saltwater extracted are implemented.
- The low permeable barrier wall located closer to the *PW* is effective in reducing the $\overline{C}$ value in the *PW*.

- However it is more preferable to built an economical barrier.

In conclusion, from this study the recharge well is the best seawater control measure, but the barrier system may be useful in controlling seawater intrusion, therefore further research is being considered.

## References

[1] Bower, J.W., Motz, L.H., and Durden, D.W. (1999): Analytical solution for determining the critical condition of saltwater upconing in a leaky artesian aquifer, *Journal of Hydrology,* 221, pp. 43–54.

[2] Ghassemi, F., Chen, T.H., Jakeman A.J., and. Jacobson, G. (1993): Two and three-dimensional simulation of seawater intrusion: performances of the "SUTRA" and "HST3D" models, *AGSO Journal of Austrialian Geology and Geophysics,* 14 (2–3), pp. 219–226.

[3] Oude Essink, G.H.P. (2001): Salt Water Intrusion in a Three-dimensional Groundwater System in The Netherlands: A Numerical Study, *Transport in Porous Media*, 43 (1), pp. 137-158.

[4] Oude Essink G.H.P. (1996): Impact of sea level rise on groundwater flow regimes, PhD Thesis, Delft University of Technology, The Netherlands.

[5] Reilly, T.E., and Goodman, A.S. (1987): Analysis of saltwater upconing beneath a pumping well, *Journal of Hydrology,* 89, pp. 169–204.

[6] Todd, D.K. (1974): Saltwater Intrusion and Its Control: Water Technology Resources, *Journal of American Water Works Association*, 66(3), 180- 187.

[7] Van Dam, J.C. (1997): Saltwater intrusion in coastal aquifers, guidelines for studying, monitoring, and controlling, *water reports* 11, FAO, Rome, pp.1–152.

Discussion open until June 30, 2009